Nuclear Engineering and Technology xxx (2017) 1–9

Contents lists available at ScienceDirect

Nuclear Engineering and Technology

journal homepage: www.elsevier.com/locate/net

Original Article

ENTROPY ANALYSIS IN A CILIA TRANSPORT OF NANOFLUID UNDER THE INFLUENCE OF MAGNETIC FIELD

MUHAMMAD N. ABRAR [A, B, *], RIZWAN UL HAQ [C], MUHAMMAD AWAIS [D], IRFAN RASHID [A]

[a] Department of Mathematics, Capital University of Science and Technology, Zone V Express way, Islamabad 44000, Pakistan
[b] DBS-H, CECOS University of Information Technology and Emerging Sciences, Phase VI Hayatabad, Peshawar 25000, Pakistan
[c] Department of Electrical Engineering, Bahria University, Shangrilla Road, Sector E-8, Islamabad 44000, Pakistan
[d] Department of Mathematics, COMSATS Institute of Information Technology, Kamra Road, Attock 43600, Pakistan

ARTICLE INFO

Article history:
Received 25 June 2017
Received in revised form
29 August 2017
Accepted 17 September 2017
Available online xxx

Keywords:
Angle of Inclination
Ciliated Walls and Magnetic Field
Entropy Analysis
Viscous Dissipation

ABSTRACT

In this study, analysis is performed on entropy generation during cilia transport of water based titanium dioxide nanoparticles in the presence of viscous dissipation. Moreover, thermal heat flux is considered at the surface of a channel with ciliated walls. Mathematical formulation is constructed in the form of nonlinear partial differential equations. Making use of suitable variables, the set of partial differential equations is reduced to coupled nonlinear ordinary differential equations. Closed form exact solutions are obtained for velocity, temperature, and pressure gradient. Graphical illustrations for emerging flow parameters, such as Hartmann number (Ha), Brinkmann number (Br), radiation parameter (Rn), and flow rate, have been prepared in order to capture the physical behavior of these parameters. The main goal (i.e., the minimizing of entropy generation) of the second law of thermodynamics can be achieved by decreasing the magnitude of Br, Ha and Λ parameters.

1. Introduction

In the last several decades, a number of techniques have been introduced by scientists to boost the efficiency of heat transfer. In this regard, scientists have introduced wavy surfaces, micro channels, and vibration phenomena to heat transfer surfaces. However, the rate of heat transfer can also be upgraded by strengthening the thermal conductivity of conventional fluids. As conventional fluids, such as water, engine oil, lubricants etc., retain limited heat transfer abilities because of low thermal conductivity, they are not capable of meeting modern age cooling needs. On the other side, nanoparticles have dramatically higher thermal conductivity than that of pure fluids. Currently, titanium dioxide has seen potential application in skin care products, cosmetic, sunscreens, etc. Sunscreens are used to protect skin tissues from the harmful radiation of sun. Furthermore, they also reduce the probability of skin tumors, skin smolder, and untimely maturing.

The strength of the thermal nature of nanofluids has key importance in medical science and engineering fields including power generation, transportation, micromanufacturing, pharmaceutical processes, air-conditioning, etc. To be specific, let us consider nanoparticles: titanium dioxide (TiO_2) nanoparticles achieve their best performance in biological, chemical, and environmental engineering, for instance, in drugs, foodstuff, skin goods, toothpastes, paints, nail polishes, plastics, printing inks, and ceramic glazes; these nanoparticles have great potential for remediation of waste water. Based on the above applications of nanoparticles, Choi [1] initially came up with the concept of nanofluids and verified his theory experimentally. Several studies in this direction have been undertaken using different flow conditions: flow induced by linear stretching with convective heating was presented by Makinde and Aziz [2]; stagnation point flow under the influence of porous medium was studied by Alsaedi et al. [3]; Brownian motion and thermophoresis effects over an exponential stretching surface were demonstrated by Nadeem and Lee [4]; characteristics of unsteady flow past an infinite vertical plate were examined by Turkyilmazoglu and Pop [5]; natural convection flow under the action of Lorentz forces was discussed by Sheikholeslami et al. [6]; third grade nanofluid flow in the presence of magnetic field and the Maxwell model for convective cooling were studied by Awais et al. [7,8]; consequences of forced convection

* *Corresponding author.*
E-mail address: nasirabrar10@gmail.com (M.N. Abrar).

https://doi.org/10.1016/j.net.2017.09.007

Nomenclature

nf	Nanofluid
β	Wave number
p	Solid nanoparticles
Θ	Angle of inclination
θ	Dimensionless temperature
Ω	Heat absorption parameter
σ^*	Stefan–Boltzmann constant
ρ_{nf}	Effective density of the nanofluid
ρC_p	Thermal conductivity of the fluid
φ	Solid volume fraction of nanofluid
λ	Wavelength of the metachronal wave
Λ	Dimensionless temperature difference
k_{bf}	Thermal conductivity of the base fluid
ε	Non-dimensional measure with respect to cilia length
μ_{nf}	Effective dynamic viscosity of the nanofluid
α	Measure of the eccentricity of the elliptical motion
bf	Base fluid
B_0	Magnetic field
Gr	Grashof number
Ns	Entropy number
Ha	Hartmann number
$\hbar$	Height of the tube
Rn	Radiation parameter
w	Dimensionless velocity
e	Mean radius of the tube
α_{nf}	Effective thermal diffusivity
k_{nf}	Effective thermal conductivity
$\tilde{T}$	Local temperature of the fluid
$\widetilde{Z_0}$	Reference position of the particle
Q_0	Dimensional heat absorption effect
c	Wave speed of the metachronal wave
k^*	Rosseland mean absorption coefficient

heat transfer in a lid driven semi annuls and natural convection heat transfer in a cubic cavity was presented Sheikholeslami et al. [9,10]; impulsive motion of free convective flow under the influence of thermal heat flux was studied by Das and Jana [11]; mixed convection flow in a symmetric channel was analyzed by Abbasi et al. [12]; and impact of thermal radiation in a stretching cylinder was demonstrated by Hayat et al. [13]. Apart from peristaltic studies, some of the latest studies that deal with magneto-hydrodynaimics (MHD) effects for both Newtonian and non-Newtonian fluid are analyzed for various kinds of stretching sheet [14–23].

At present, all heat transfer mechanisms generate entropy. The magnetic, viscous, heat transfer, fall temperature gradient, etc., properties are responsible for the generation of entropy. The entropy generation is associated with the number of energy-related applications such as geothermal power systems, cooling of modern electronic systems, and solar power collectors. Initially, Bejan [24] proposed the theory of entropy generation in heat transfer and fluid flow systems. Some relevant studies on the subject can be seen in the list of references Pakdemirli and Yilbas [25], Aiboud and Saouli [26], Rashidi et al. [27], Galanis and Rashidi [28], Rashidi et al. [29], Ellahi et al. [30], Bhatti et al. [31] and Jamalabadi et al. [32].

The primary focus of this study is to analyze entropy generation during cilia transport under the influence of thermal heat flux and viscous dissipation. In the next sections, author provides an analysis of the problem. Section 3 gives the formulation of entropy generation. An exact solution in closed form for the velocity, temperature, and pressure gradients is presented in Section 4. In Section 5, we discuss the physical sense of the problem through plots and tables. The last section includes the final outcomes of the present study.

2. Analysis

Let us consider ciliary transport of two dimensional, incompressible, and axisymmetric flow of a titanium dioxide water nanofluid in a horizontal tube. The inner surface of the tube is ciliated with metachronal waves. Flow is provoked as a result of these metachronal waves, which are formed due to collective beating of the cilia with constant momentum along the walls of the body. Uniform magnetic field is applied at the angle of inclination (Θ). Heat transfer analysis with the viscous dissipation is also considered. Fig. 1 shows the physical view of the presented model and the coordinates system. The horizontal and vertical velocities of the cilia are given as [33,34]:

$$\tilde{W} = \frac{\left(\frac{-2\pi}{\lambda}\right)\left[ce\varepsilon\alpha\cos\left(\frac{2\pi}{\lambda}\left(\tilde{Z}-c\tilde{t}\right)\right)\right]}{1-\frac{2\pi}{\lambda}\left[e\varepsilon\alpha\cos\left(\frac{2\pi}{\lambda}\left(\tilde{Z}-c\tilde{t}\right)\right)\right]}, \tag{1}$$

$$\tilde{U} = \frac{\left(\frac{2\pi}{\lambda}\right)\left[ce\varepsilon\alpha\sin\left(\frac{2\pi}{\lambda}\left(\tilde{Z}-c\tilde{t}\right)\right)\right]}{1-\frac{2\pi}{\lambda}\left[e\varepsilon\alpha\cos\left(\frac{2\pi}{\lambda}\left(\tilde{Z}-c\tilde{t}\right)\right)\right]}. \tag{2}$$

The following transformation is useful to switch the flow from fixed frame to wave frame.

$$\tilde{r} = \tilde{R}, \quad \tilde{z} = \tilde{Z} - c\tilde{t}, \quad \tilde{u} = \tilde{U}, \quad \tilde{w} = \tilde{W} - c. \tag{3}$$

The fundamental governing equations in the fixed frame for an incompressible nanofluid can be written as:

$$\frac{\partial\tilde{u}}{\partial\tilde{r}} + \frac{\tilde{u}}{\tilde{r}} + \frac{\partial\tilde{w}}{\partial\tilde{z}} = 0, \tag{4}$$

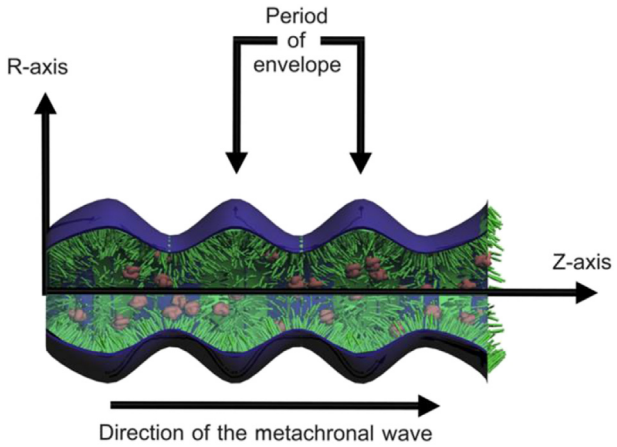

Fig. 1. Geometry of the problem.

Please cite this article in press as: M.N. Abrar, et al., ENTROPY ANALYSIS IN A CILIA TRANSPORT OF NANOFLUID UNDER THE INFLUENCE OF MAGNETIC FIELD, Nuclear Engineering and Technology (2017), https://doi.org/10.1016/j.net.2017.09.007

$$\rho_{nf}\left[\tilde{u}\frac{\partial\tilde{u}}{\partial\tilde{r}}+\tilde{u}\frac{\partial\tilde{w}}{\partial\tilde{z}}\right]=-\frac{\partial\tilde{p}}{\partial\tilde{r}}+2\mu_{nf}\left[\frac{\partial^2\tilde{u}}{\partial\tilde{r}^2}\right]+\mu_{nf}\frac{2}{\tilde{r}}\left[\frac{\partial\tilde{u}}{\partial\tilde{r}}-\frac{\tilde{u}}{\tilde{r}}\right]+\mu_{nf}\left[\frac{\partial^2\tilde{u}}{\partial\tilde{z}\partial\tilde{r}}+\frac{\partial^2\tilde{w}}{\partial\tilde{z}^2}\right],\tag{5}$$

$$\rho_{nf}\left[\tilde{u}\frac{\partial\tilde{w}}{\partial\tilde{r}}+\tilde{w}\frac{\partial\tilde{w}}{\partial\tilde{z}}\right]=-\frac{\partial\tilde{p}}{\partial\tilde{z}}+2\mu_{nf}\left[\frac{\partial^2\tilde{w}}{\partial\tilde{z}^2}\right]+\mu_{nf}\left[\frac{1}{\tilde{r}}\left(\frac{\partial\tilde{u}}{\partial\tilde{z}}+\frac{\partial\tilde{w}}{\partial\tilde{r}}\right)+\frac{\partial}{\partial\tilde{r}}\left(\frac{\partial\tilde{u}}{\partial\tilde{z}}+\frac{\partial\tilde{w}}{\partial\tilde{r}}\right)\right]-\sigma_{nf}B_0^2cos(\Theta)(\tilde{w}+c),\tag{6}$$

$$(\rho C)_{nf}\left[\tilde{u}\frac{\partial\tilde{T}}{\partial\tilde{r}}+\tilde{w}\frac{\partial\tilde{T}}{\partial\tilde{z}}\right]=+k_{nf}\left[\frac{1}{\tilde{r}}\frac{\partial}{\partial\tilde{r}}\left(\tilde{r}\frac{\partial\tilde{T}}{\partial\tilde{r}}\right)+\frac{\partial^2\tilde{T}}{\partial\tilde{z}^2}\right]+Q_0+\frac{16\sigma^*T_\infty^3}{3k^*}\left[\frac{1}{\tilde{r}}\frac{\partial}{\partial\tilde{r}}\left(\tilde{r}\frac{\partial\tilde{T}}{\partial\tilde{r}}\right)\right]+\mu_{nf}\left[2\left(\frac{\partial\tilde{u}}{\partial\tilde{z}}\right)^2+2\left(\frac{\partial\tilde{w}}{\partial\tilde{r}}\right)^2+\left(\frac{\partial\tilde{u}}{\partial\tilde{r}}+\frac{\partial\tilde{w}}{\partial\tilde{z}}\right)^2\right],\tag{7}$$

where, $\tilde{u}$ and $\tilde{w}$ are the velocity elements in the $\tilde{r}$ and $\tilde{z}$ directions, respectively. Further, B_0 represents the magnetic field, σ the electrical conductivity, $\tilde{T}$ the local temperature of the fluid, Q_0 the dimensional heat absorption coefficient, σ^* the Stefan–Boltzmann constant, and k^* the Rosseland mean absorption coefficient. Further, the physical properties of the nanofluid, including thermal diffusivity, viscosity, density, heat capacitance, and thermal conductivity are defined as follows [35]:

$$\alpha_{nf}=\frac{k_{nf}}{(\rho C)_{nf}},$$

$$\mu_{nf}=\frac{\mu_{bf}}{(1-\varphi)^{2.5}},$$

$$\rho_{nf}=(1-\varphi)\rho_{bf}+\varphi\rho_p,$$

$$\rho_{nf}=\frac{(1-\varphi)(\rho C)_{bf}+\varphi(\rho C)_p}{(C)_{nf}},$$

$$k_{nf}=\frac{k_p+2k_{bf}+2\left(k_p-k_{bf}\right)\varphi(1+\gamma)^3}{k_p+2k_{bf}-2\left(k_p-k_{bf}\right)\varphi(1+\gamma)^3}k_{bf},\tag{8}$$

where, the subscripts p, bf and nf indicate the solid nanoparticles, base fluid, and nanofluid, respectively. Further, γ represents the ratio of the nanolayer thickness to the original particle radius.

We introduce the following nondimensional variables to make the system dimensionless.

$$r=\frac{\tilde{r}}{e},\quad z=\frac{\tilde{z}}{\lambda},\quad u=\frac{\lambda\tilde{u}}{ec},\quad p=\frac{e^2\tilde{p}}{c\lambda\mu_{bf}},\quad h=\frac{\hbar}{e}=1+\varepsilon\cos(2\pi z),$$
$$Re=\frac{e\rho_{nf}}{\mu_{nf}},\quad w=\frac{\tilde{w}}{c},\quad \delta=\frac{e}{\lambda},\quad Ha^2=\frac{e^2B_0^2\sigma_{nf}}{\mu_{bf}},\quad \Omega=\frac{Q_0e^2}{k_{bf}\widetilde{T_0}},$$
$$\theta=\frac{\left(\tilde{T}-\widetilde{T_0}\right)}{\widetilde{T_0}},\quad Br=\frac{c^2\mu_{bf}}{k_{bf}\widetilde{T_0}},\quad Rn=\frac{16\sigma^*}{3k^*k_{bf}}T_\infty^3.\tag{9}$$

By considering the above nondimensional variables in Eqs. (4)–(7) and employing the supposition of low Reynolds number ($Re\ll1$) and long wavelength ($\delta\to0$), the nondimensional equations can be written as:

$$\frac{dp}{dr}=0,\tag{10}$$

$$\frac{dp}{dz}-\frac{1}{(1-\varphi)^{2.5}}\left(\frac{1}{r}\frac{dw}{dr}+\frac{d^2w}{dr^2}\right)+Ha^2cos(\Theta)(w+1)=0,\tag{11}$$

$$\left(1+\frac{Rn}{\Psi_{10}}\right)\left(\frac{d^2\theta}{dr^2}+\frac{1}{r}\frac{d\theta}{dr}\right)+\frac{1}{\Psi_{10}}\frac{Br}{(1-\varphi)^{2.5}}\left(\frac{dw}{dr}\right)^2+\Omega=0.\tag{12}$$

The convenient boundary conditions on the ciliated walls are given as:

$$\frac{\partial w}{\partial r}=0,\quad \frac{\partial\theta}{\partial r}=0,\quad at\quad r=0,\tag{13}$$

$$w=\frac{-2\pi\varepsilon\alpha\beta\cos(2\pi z)}{1-2\pi\varepsilon\alpha\beta\cos(2\pi z)}-1,\quad \theta=0\quad at\quad r=\hbar(z)=1+\varepsilon\cos(2\pi z).\tag{14}$$

The volumetric entropy generation term $\widehat{S}_{gen}$ can be calculated as follows:

$$\widehat{S}_{gen}=\frac{k_{nf}}{\widetilde{\theta_0^2}}\left(\left(\frac{\partial\tilde{T}}{\partial\tilde{r}}\right)^2+\left(\frac{\partial\tilde{T}}{\partial\tilde{z}}\right)^2\right)+\frac{\tilde{\Phi}}{\widetilde{\theta_0}}+\frac{\sigma B_0^2}{\widetilde{\theta_0}}\cos(\Theta)(\tilde{w}+c)^2.\tag{15}$$

The dimensional viscous dissipation term $\tilde{\Phi}$ is given as:

$$\tilde{\Phi}=\mu_{nf}\left[2\left(\frac{\partial\tilde{u}}{\partial\tilde{z}}\right)^2+2\left(\frac{\partial\tilde{w}}{\partial\tilde{r}}\right)^2+\left(\frac{\partial^2\tilde{u}}{\partial\tilde{r}}+\frac{\partial^2\tilde{w}}{\partial\tilde{z}}\right)^2\right],\tag{16}$$

whereas, the dimensionless entropy generation rate (Ns) is given as:

$$Ns=\frac{\widehat{S}_{gen}}{\widehat{S}_{Gen}}=\frac{k_{nf}}{k_{bf}}\left(\frac{\partial\theta}{\partial r}\right)^2+\Lambda Br\left(\frac{\mu_{nf}}{\mu_{bf}}\right)\cdot\left(\frac{\partial w}{\partial r}\right)^2+\Lambda BrHa^2\cos(\Theta)(w+1)^2,\tag{17}$$

or

Please cite this article in press as: M.N. Abrar, et al., ENTROPY ANALYSIS IN A CILIA TRANSPORT OF NANOFLUID UNDER THE INFLUENCE OF MAGNETIC FIELD, Nuclear Engineering and Technology (2017), https://doi.org/10.1016/j.net.2017.09.007

$$Ns = N_H + N_V + N_M \tag{18}$$

Eq. (17) clearly displays the three different roots for the generation of entropy:

1st term appears due to heat transfer (N_H) irreversibility.
2nd term appears because of the presence of viscous dissipation (N_V) effect.
3rd term turns out to be due to the response of the magnetic field (N_M).

The characteristic entropy generation, finite temperature difference, and Hartman number (Ha) are given, respectively, as:

$$\widehat{S}_{Gen} = \frac{k_{bf}\tilde{T}_0^2}{\tilde{\theta}_0^2 a_1^2}, \quad \Lambda = \frac{\tilde{\theta}_0}{\tilde{T}_0}, \quad Ha^2 = \frac{e^2 B_0^2 \sigma_{nf}}{\mu_{bf}}. \tag{19}$$

To evaluate the irreversibility distribution, another parameter, Bejan number (Be), which is the ratio of the heat transfer irreversibility to total irreversibility due to heat transfer, fluid friction, and magnetic field, is given as:

$$Be = \frac{N_H}{N_H + N_V + N_M} \tag{20}$$

3. Exact solutions

In this section we present the exact solutions to coupled ordinary differential Eqs. (11) and (12), together with boundary conditions (13) and (14). The interpretation of the velocity, pressure gradient, and temperature can be written as:

$$w(r,z) = \left(\frac{F\Psi_2 I_0\left[\Psi_3 Ha\sqrt{\Psi_1}\sqrt{cos\Theta}\right] - \left(\Psi_3^2 + F\Psi_2\right) I_0\left[rHa\sqrt{\Psi_1}\sqrt{cos\Theta}\right]}{\Psi_3^2\Psi_2 I_2\left[\Psi_3 Ha\sqrt{\Psi_1}\sqrt{cos\Theta}\right.}\right) + \Psi_3^2\left(\frac{{}_0\bar{F}_1\left[2, \frac{1}{4}\Psi_3^2 Ha^2\Psi_1 cos\Theta\right]}{\Psi_3^2\Psi_2 I_2\left[\Psi_3 Ha\sqrt{\Psi_1}\sqrt{cos\Theta}\right)}\right), \tag{21}$$

where, the flow rate is given by

$$Q = 2\int_0^{\hbar(z)} rw(r,z)dr, \tag{22}$$

with substitution of Eq. (21) into Eq. (22) and then solving for the result of dp/dz we havewhere, the expressions for $(\Psi_i, i = 1-10)$ are given as:

$$\frac{dp}{dz} = \frac{Ha^2\cos\Theta\left(\Psi_3^2 - F\right)\Psi_2 I_0\left(Ha\Psi_3\sqrt{\Psi_1}\sqrt{\cos\Theta}\right) + \Psi_3^2(\Psi_2 - 1){}_0\bar{F}_1\left[2, \frac{1}{4}\Psi_3^2\Psi_1\cos\Theta\right]}{\Psi_3^2 I_2\left[\Psi_3 Ha\sqrt{\Psi_1}\sqrt{\cos\Theta}\right]\Psi_2}, \tag{23}$$

$$\theta(r,z) = \frac{\left(Br\left(\Psi_3^2 + F\Psi_2\right)^2\left(\Psi_4 + Ha^2\Psi_1\left(-\Psi_3^2(\Psi_5\Psi_6) + r^2(\Psi_7\Psi_8)\right)\cos\Theta\right) + \Psi_9\right)}{\left(4\Psi_3^4\Psi_2^2\Psi_1 I_2\left[hHa\sqrt{\Psi_1}\sqrt{\cos\Theta}\right]^2(Rn + \Psi_{10})\right)}, \tag{24}$$

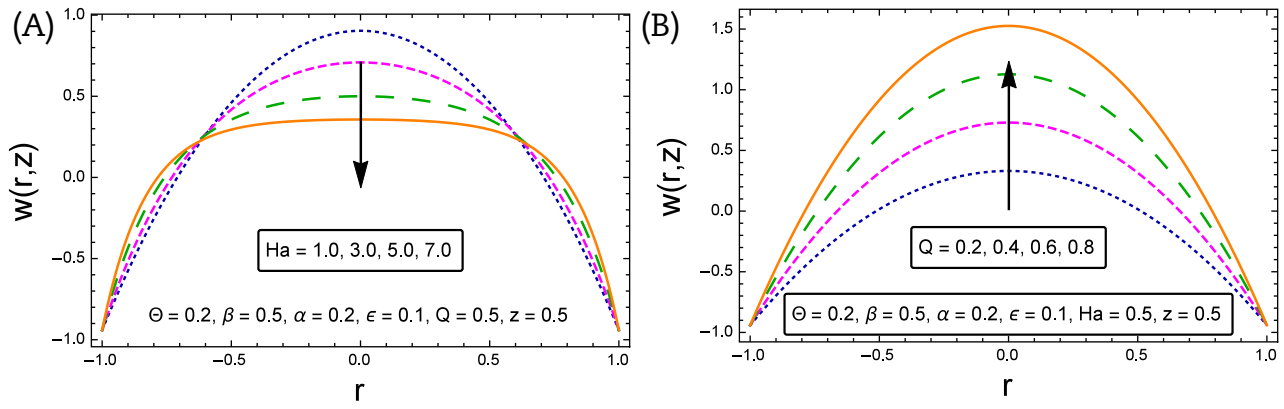

Fig. 2. (A) Response of Ha on $w(r,z)$ for different flow parameters. (B) Response of Q at $w(r,z)$ for different flow parameters. Ha, Hartman number; Q, flow rate.

Please cite this article in press as: M.N. Abrar, et al., ENTROPY ANALYSIS IN A CILIA TRANSPORT OF NANOFLUID UNDER THE INFLUENCE OF MAGNETIC FIELD, Nuclear Engineering and Technology (2017), https://doi.org/10.1016/j.net.2017.09.007

$$\Psi_1 = (1-\varphi)^{2.5},$$

$$\Psi_2 = 1 - 2\pi\varepsilon\alpha\beta\cos[2\pi z],$$

$$\Psi_3 = 1 + \varepsilon\cos[2\pi z],$$

$$\Psi_4 = 2I_0\left[\Psi_3 Ha\sqrt{\Psi_1}\sqrt{\cos\Theta}\right]^2 - 2I_0\left[rHa\sqrt{\Psi_1}\sqrt{\cos\Theta}\right]^2,$$

$$\Psi_5 = -2I_1\left[\Psi_3 Ha\sqrt{\Psi_1}\sqrt{\cos\Theta}\right] + 2I_0\left[\Psi_3 Ha\sqrt{\Psi_1}\sqrt{\cos\Theta}\right],$$

$$\Psi_6 = \left(I_0\left[\Psi_3 Ha\sqrt{\Psi_1}\sqrt{\cos\Theta}\right] + I_2\left[\Psi_3 Ha\sqrt{\Psi_1}\sqrt{\cos\Theta}\right]\right),$$

$$\Psi_7 = -2I_1\left[rHa\sqrt{\Psi_1}\sqrt{\cos\Theta}\right]^2 + 2I_0\left[rHa\sqrt{\Psi_1}\sqrt{\cos\Theta}\right]^2,$$

$$\Psi_8 = \left(I_0\left[rHa\sqrt{\Psi_1}\sqrt{\cos\Theta}\right] + 2I_2\left[rHa\sqrt{\Psi_1}\sqrt{\cos\Theta}\right]\right),$$

$$\Psi_9 = \Psi_3^4\left(\Psi_3^2 - r^2\right)\Psi_1\Psi_2\Omega I_2\left[\Psi_3 Ha\sqrt{\Psi_1}\sqrt{\cos\Theta}\right]^2\Psi_{10},$$

$$\Psi_{10} = \frac{k_p + 2k_{bf} + 2\left(k_p - k_{bf}\right)\varphi(1+\gamma)^3}{k_p + 2k_{bf} - 2\left(k_p - k_{bf}\right)\varphi(1+\gamma)^3}. \tag{25}$$

Setting the mean flow rate equal to:

$$F = Q - \left[0.5 + \frac{\varepsilon^2}{4}\right], \tag{26}$$

the pressure rise can be calculated as:

$$\Delta P = \int_0^1 \frac{dp}{dz}dz. \tag{27}$$

4. Results and discussion

The main interest here is to study the effects of Hartman number (Ha), flow rate (Q), radiation parameter (Rn), Brinkmann number (Br), angle of inclination (Θ), wave number (β) and cilia length (ε) on the velocity field $w(r,z)$, temperature field $\theta(r,z)$, pressure gradient (ΔP), entropy number (Ns), and Bejan number (Be). For this purpose, the velocity field is plotted against the radial

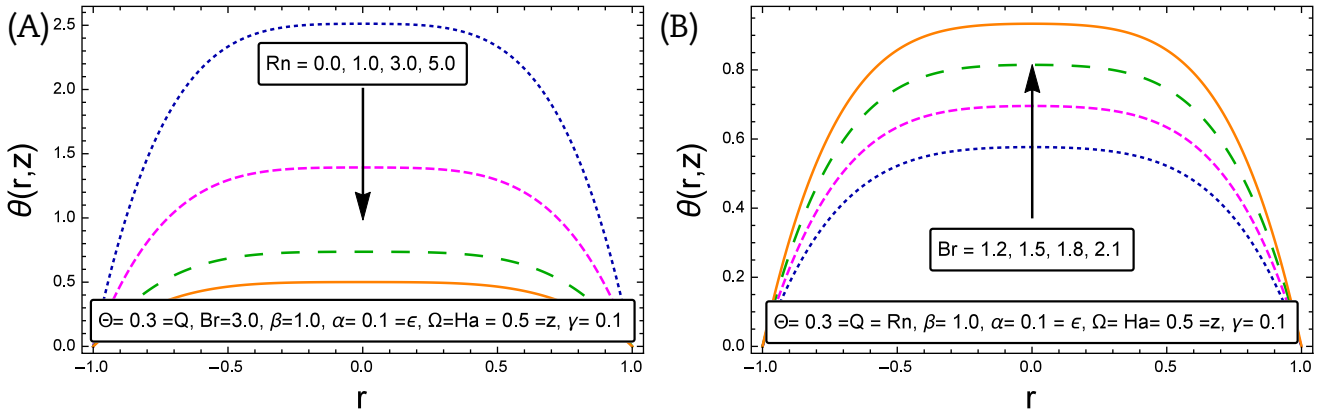

Fig. 3. (A) Response of Rn at θ for different flow parameters. (B) Response of Br at θ for different flow parameters. Rn, radiation parameter; Br, Brinkmann number.

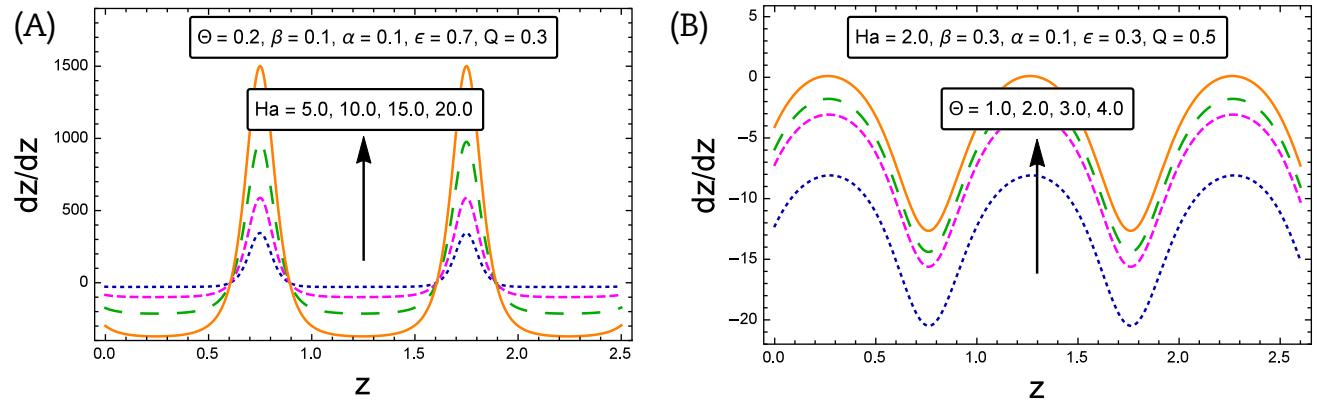

Fig. 4. (A) Response of Ha at dp/dz for different flow parameters. (B) Response of Θ at dp/dz for different flow parameters. Ha, Hartman number; Θ, angle of inclination.

Please cite this article in press as: M.N. Abrar, et al., ENTROPY ANALYSIS IN A CILIA TRANSPORT OF NANOFLUID UNDER THE INFLUENCE OF MAGNETIC FIELD, Nuclear Engineering and Technology (2017), https://doi.org/10.1016/j.net.2017.09.007

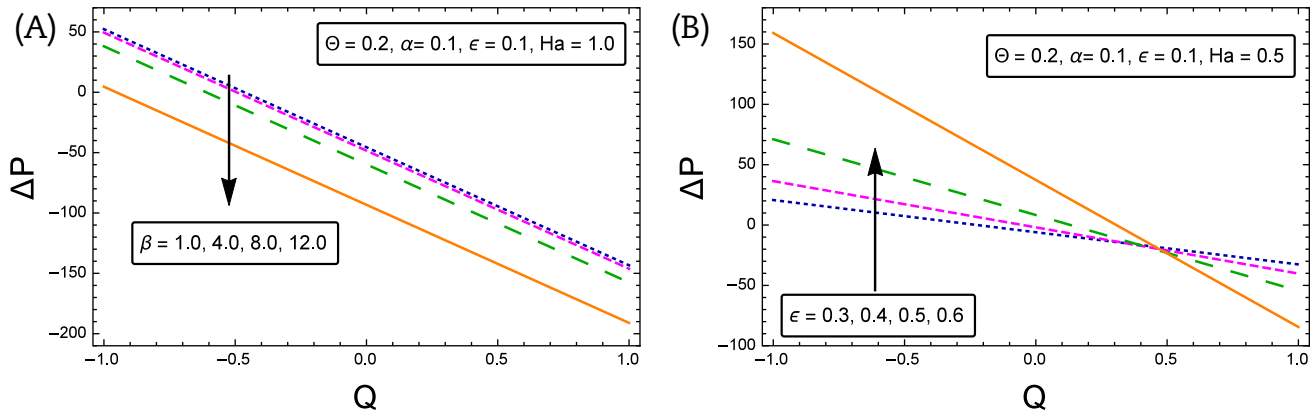

Fig. 5. (A) Response of β at ΔP for different flow parameters. (B) Response of ε at ΔP for different flow parameters. β, wave number; ε, cilia length; ΔP, pressure rise.

distance (r) for different values of *Ha* and *Q*. Fig. 2A clearly shows that as *Ha* increases, the fluid velocity decreases due to the fact that viscous forces are highly dominant against the electromagnetic forces, which retard the flow. It can be seen that velocity is at its maximum at $r = 0$ and the velocity starts to decrease near the ciliated walls. Fig. 2B shows that for increasing values of *Q*, the velocity of the fluid increases rapidly, if other parameters are kept fixed. The fluid velocity is at its maximum at the center of the tube and at its minimum near the ciliated walls, which are influenced by cilia motion. The temperature profile is portrayed in Fig. 3A and B in the radial direction for increasing values of the radiation parameter (Rn) and the Brinkmann number (Br). It is illustrated in Fig. 3A that by increasing the magnitude of the radiation number (Rn) the temperature of the fluid starts to decrease. An increase in *Rn* means a decrease in the mean absorption parameter, which refers to the fact that less energy is absorbed by the fluid. On the other side, the temperature of the fluid significantly increases for higher values of Brinkman number (see Fig. 3B). This behavior is obvious, as Brinkmann number *Br* describes the conduction of heat from a wall to a flowing viscous fluid. Therefore, as *Br* increases, the temperature profile also increases.

Fig. 4A and 4B show the effects of the pressure gradient (dp/dz) vs. the axial direction (z) for different flow parameters. Pressure gradient is a local characterization of the fluid under investigation and is responsible for the fluid circulation. We notice that the rise in *Ha* increases the pressure gradient (see Fig. 4A). Similarly, an increase in angle of the inclination (Θ) causes more rapid flow, which implies high pressure gradient. The behavior changes with increases in Θ, as the increase of this value produces an increment in the pressure gradient. Fig. 5A and 5B show the variation of the

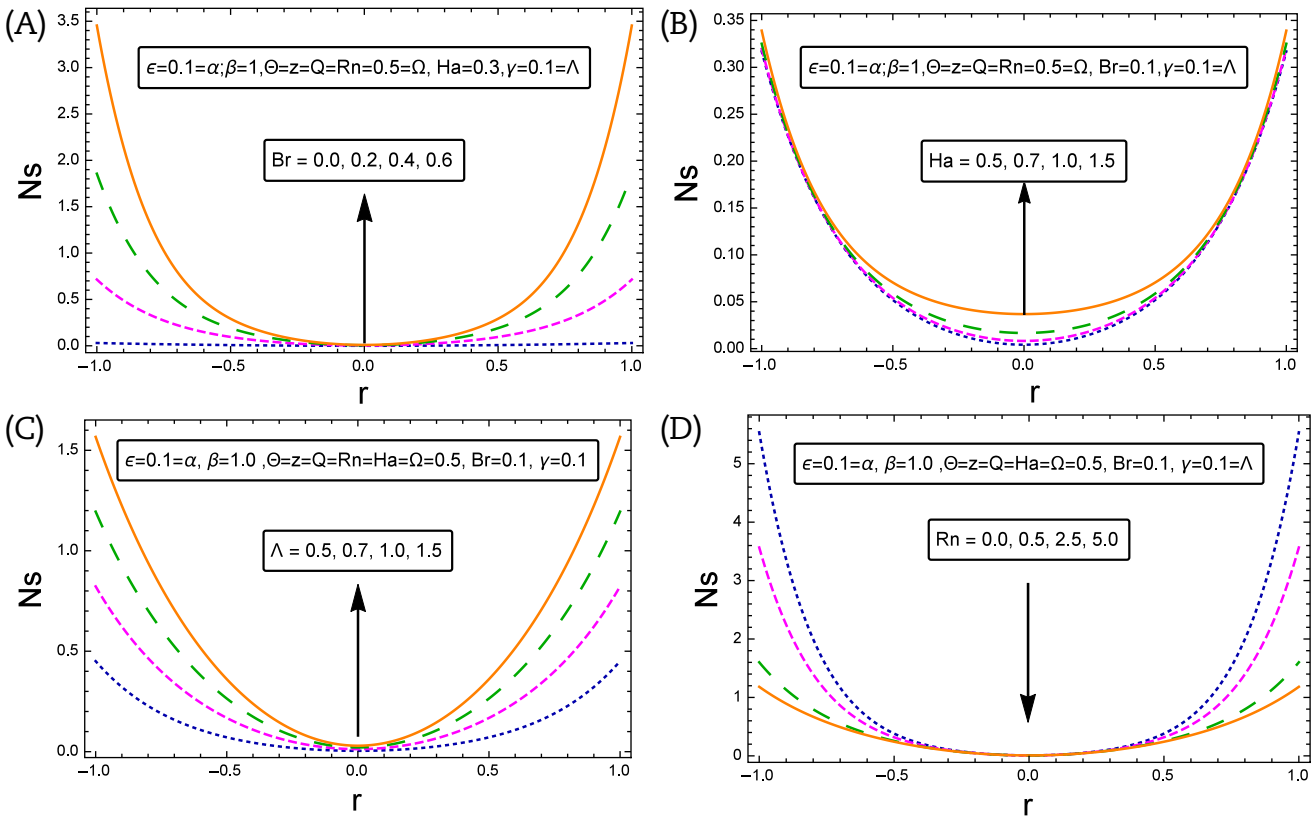

Fig. 6. (A) Response of *Br* at *Ns* for different flow parameters. (B) Response of *Ha* at *Ns* for different flow parameters. (C) Response of Λ at *Ns* for different flow parameters. (D) Response of *Rn* at *Ns* for different flow parameters. *Br*, Brinkmann number; *Ha*, Hartman number; *Ns*, entropy number; *Rn*, radiation parameter; Λ, dimensionless temperature difference.

Please cite this article in press as: M.N. Abrar, et al., ENTROPY ANALYSIS IN A CILIA TRANSPORT OF NANOFLUID UNDER THE INFLUENCE OF MAGNETIC FIELD, Nuclear Engineering and Technology (2017), https://doi.org/10.1016/j.net.2017.09.007

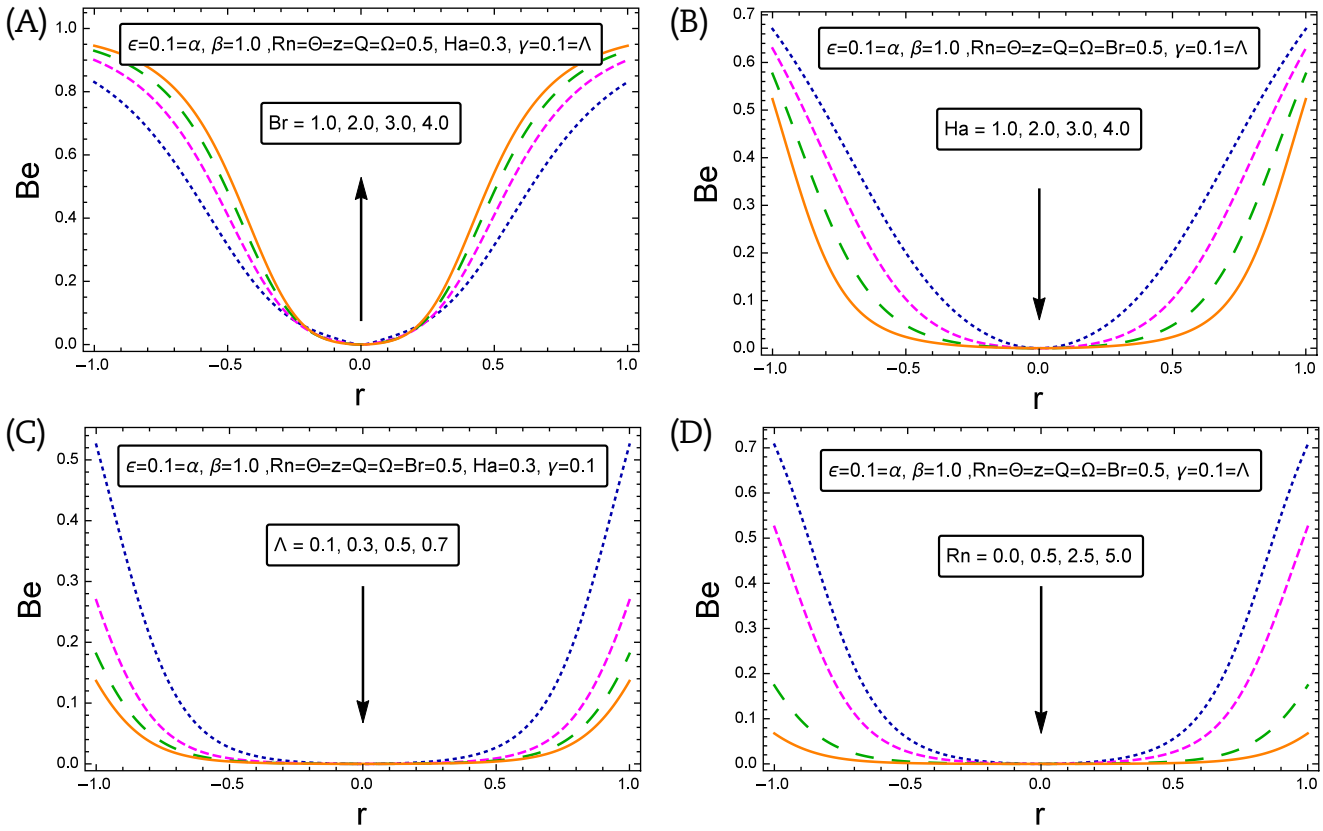

Fig. 7. (A) Response of *Br* at *Be* for different flow parameters. (B) Response of *Ha* at *Be* for different flow parameters. (C) Response of Λ at *Be* for different flow parameters. (D) Response of *Rn* at *Be* for different flow parameters. *Be*, Bejan number; *Br*, Brinkmann number; *Ha*, Hartman number; *Rn*, radiation parameter; Λ, dimensionless temperature difference.

pressure rise (ΔP) vs. the flow rate (Q) for the flow parameter wave number (β) and the nondimensional measure of cilia length (ε). Fig. 5A shows that an increase in the wave number (β) results in a decrease of the pressure rise when keeping other parameters constant. Fig. 5B shows that pressure rise is directly proportional to the nondimensional parameter ε. When ε rises, the fluid has more ability to flow, and so pressure rises with the increase in ε in the peristaltic pumping $\Delta P > 0$ region and decreases in the augmented pumping region $\Delta P < 0$. The thermophysical properties, for titatnium dioxide and water are listed in Table 1.

Table 1
Thermophysical properties of titanium dioxide (TiO_2) and water (H_2O) [36].

Item	ρ (kg/m^3)	C_p (J/kg K)	K (W/m K)
TiO_2	4250.0	686.2	8.9538
H_2O	997.1	4179.0	0.613

4.1. Entropy analysis and streamlines

Fig. 6A–D were developed to show the physical behavior of entropy in the radial direction for different parameters, i.e., Brinkman number, Hartman number, dimensionless temperature difference (Λ), and radiation parameter. Fig. 6A–C show that by increasing the *Br*, *Ha*, and Λ, the entropy number also increases. As *Br* increases, heat transfer dominates fluid viscosity within the channel, which causes increase of the entropy. Small entropy is recorded at the bottom of the tube and larger entropy is recorded near the ciliated walls in all cases. The influence of the thermal radiation is demonstrated in Fig. 6D. It can be observed that with an increase in $Rn = (0.0, 1.0, 2.0, 3.0)$, the entropy number decreases, but the values are almost same at the bottom of tube. From the graphical illustration, it is quite clear that the entropy number is directly proportional to the Hartman number, Brinkman number, and dimensionless temperature difference, and

Table 2
Variation in entropy generation number for various values of radiation parameter *Rn* and solid volume fraction of nanofluid while setting other particulars constant ($z = 0.5, \varepsilon = 0.1, e = 0.5, Q = 0.5, Ha = 0.5, \gamma = 1.0, \beta = 1.0, \Theta = 0.1, \Lambda = 0.1, \Omega = 0.5, Br = 1.0$).

Rn	φ	$r = \pm 1.0$	$r = \pm 0.75$	$r = \pm 0.5$	$r = \pm 0.25$
0.0	0.0	15.66690	3.52975	0.68267	0.13833
1.0		04.99361	1.48760	0.45298	0.12839
2.0		03.01717	1.10985	0.41045	0.12644
3.0		02.32539	0.97751	0.39557	0.12578
0.0	0.1	00.86073	1.01024	0.46434	0.13054
1.0		00.52566	0.99819	0.45824	0.12351
2.0		−00.01107	0.97891	0.44845	0.11225
3.0		−00.95100	0.94513	0.43133	0.09254

Please cite this article in press as: M.N. Abrar, et al., ENTROPY ANALYSIS IN A CILIA TRANSPORT OF NANOFLUID UNDER THE INFLUENCE OF MAGNETIC FIELD, Nuclear Engineering and Technology (2017), https://doi.org/10.1016/j.net.2017.09.007

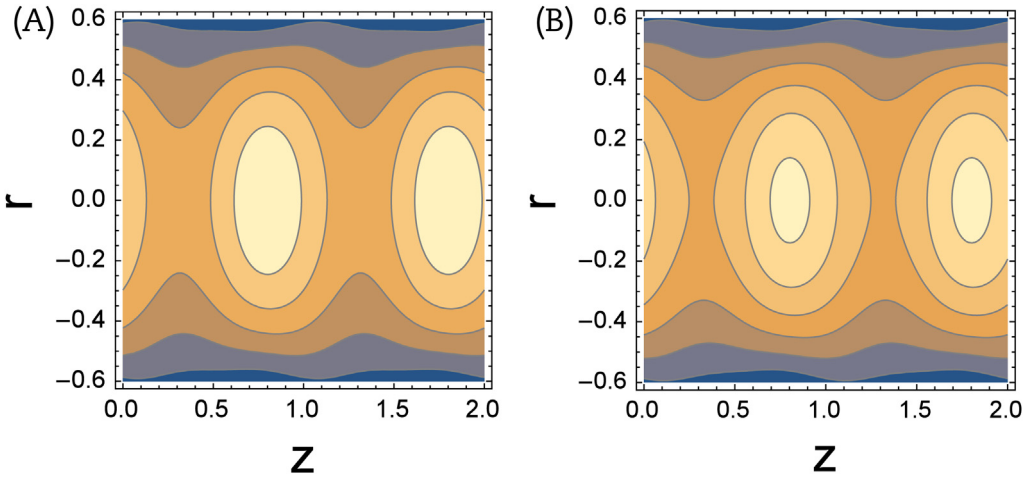

Fig. 8. (A) Streamlines for inclination angle $\Theta = 0.5$. (B) Streamlines for inclination angle $\Theta = 1.0$.

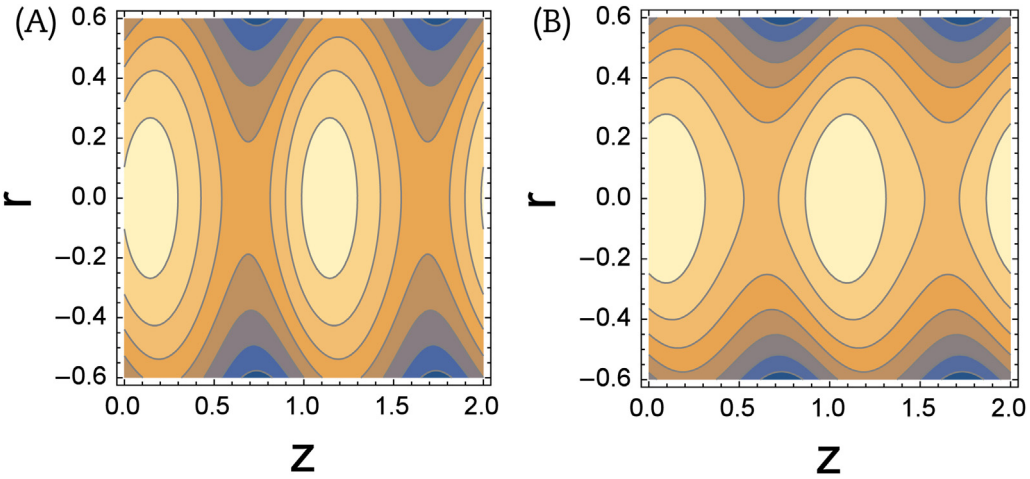

Fig. 9. (A) Streamlines for flow rate $Q = 0.1$. (B) Streamlines for flow rate $Q = 0.3$.

inversely proportional to the radiation parameter. Fig. 7A–D are prepared to illustrate the physical sense of the Bejan number (Be) against the radial distance for increasing values of Brinkman number, Hartman number, dimensionless temperature difference, and radiation parameter. It is found that Be is directly proportional to Br and inversely proportional to Ha, Λ, and Rn. The variation of entropy generation for different values of radiation parameter Rn and solid volume fraction of nanoparticle φ are presented in Table 2.

The trapping phenomenon of the streamlines of the velocity profile is shown in Figs. 8A, B and 9A, B. From Fig. 8A and B, it is clear that by increasing the inclination angle, the size of the bolus decreases, but the number of trapped boluses increases. Fig. 9A and B demonstrates that the number of trapped boluses decreases and the bolus size increases with an increment in the value of flow rate Q.

5. Conclusion

The final outcomes of the considered flow analysis are as follows:

- It is found that increasing magnitude of Hartman number retards fluid motion.
- It is acknowledged that extreme velocity happens at the center of tube and falls off near the ciliated boundary.
- It is observed that temperature profile is directly proportional to Brinkman number (Br) and inversely proportional to the radiation parameter (Rn) for fixed ratios of titanium dioxide.
- We see that Hartmann number (Ha) and angle of inclination (Θ) both are increasing function of pressure gradient.
- Rapid decline is noticed for higher magnitude of the wave number (β).
- By decreasing the magnitude of the Br, Ha and Λ parameters, we can achieve the main goal of the second law of thermodynamics, i.e., the minimizing of entropy generation.
- It is found that flow field, temperature field, and entropy generation are symmetric about the radial axis.

References

[1] S.U.S. Choi, Enhancing thermal conductivity of fluids with nanoparticle, in: D.A. Siginer, H.P. Wang (Eds.), Developments and Applications of Non-Newtonian Flows, ASME FED, 1995, pp. 99–105, 231/MD-66.
[2] O.D. Makinde, A. Aziz, Boundary layer flow of nanofluid past a stretching sheet with a convective boundary condition, Int. J. Therm. Sci. 50 (2011) 1326–1332.
[3] A. Alsaedi, M. Awais, T. Hayat, Effects of heat generation/absorption on stagnation point flow of nanofluid over a surface with convective boundary conditions, Commun. Nonlinear Sci. Numer. Simul. 17 (2012) 4210–4223.
[4] S. Nadeem, C. Lee, Boundary layer flow of nanofluid over an exponentially stretching surface, Nanoscale Res. Lett. 7 (2012) 94.
[5] M. Turkyilmazoglu, I. Pop, Heat and mass transfer of unsteady natural convection flow of some nanofluids past a vertical infinite flat plate with radiation effect, Int. J. Heat Mass Transfer 59 (2013) 167–171.

Please cite this article in press as: M.N. Abrar, et al., ENTROPY ANALYSIS IN A CILIA TRANSPORT OF NANOFLUID UNDER THE INFLUENCE OF MAGNETIC FIELD, Nuclear Engineering and Technology (2017), https://doi.org/10.1016/j.net.2017.09.007

[6] M. Sheikholeslami, M. GorjiBandpy, R. Ellahi, A. Zeeshan, Simulation of MHD CuO-water nanofluid flow and convective heat transfer considering Lorentz forces, J. Magn. Magn. Mater. 369 (2014) 69–80.
[7] M. Awais, T. Hayat, S. Iram, S. Siddiqa, A. Alsaedi, Thermophoresis and heat generation/absorption in flow of third grade nanofluid, Curr. Nanosci. 11 (2015) 394–401.
[8] M. Awais, T. Hayat, S. Iram, A. Alsaedi, Heat generation/absorption effects in a boundary layer stretched flow of Maxwell nanofluid: analytic and numeric solutions, PLoS One 10 (2015), e0129814.
[9] M. Sheikholeslami, M.M. Rashidi, D.D. Ganji, Numerical investigation of magnetic nanofluid forced convective heat transfer in existence of variable magnetic field using two phase model, J. Mol. Liq. 212 (2015) 117–126.
[10] M. Sheikholeslami, R. Ellahi, Three dimensional mesoscopic simulation of magnetic field effect on natural convection of nanofluid, Int. J. Heat Mass Transfer 89 (2015) 799–808.
[11] S. Das, R.N. Jana, Natural convective magneto-nanofluid flow and radiative heat transfer past a moving vertical plate, Alexandria Eng. J. 54 (2015) 55–64.
[12] F.M. Abbasi, T. Hayat, B. Ahmad, Peristaltic transport of an aqueous solution of silver nanoparticles with convective heat transfer at the boundaries, Can. J. Phys. 93 (2015) 1190–1198.
[13] T. Hayat, S. Asad, A. Alsaedi, Flow of Casson fluid with nanoparticles, Appl. Math. Mech. Engl. Ed. 37 (2016) 459–470.
[14] A. Shahzad, R. Ali, Approximate analytic solution for magneto-hydrodynamic flow of a non-Newtonian fluid over a vertical stretching sheet, Can. J. Appl. Sci. 2 (2012) 202–215.
[15] A. Shahzad, R. Ali, MHD flow of a non-Newtonian power law fluid over a vertical stretching sheet with the convective boundary condition, Walailak J. Sci. Technol. 10 (2012) 43–56.
[16] M. Khan, R. Ali, A. Shahzad, MHD Falkner-Skan flow with mixed convection and convective boundary conditions, Walailak J. Sci. Technol. 10 (2013) 517–529.
[17] J. Ahmed, A. Shahzad, M. Khan, R. Ali, A note on convective heat transfer of an MHD Jeffrey fluid over a stretching sheet, AIP Adv. 5 (2015) 117117.
[18] J. Ahmed, A. Begum, A. Shahzad, R. Ali, MHD axisymmetric flow of power-law fluid over an unsteady stretching sheet with convective boundary conditions, Results Phys. 6 (2016) 973–981.
[19] H. Ali, M. Khan, A revised model to analyze the heat and mass transfer mechanisms in the flow of Carreau nanofluids, Int. J. Heat Mass Transfer 103 (2016) 291–297.
[20] H. Ali, M. Khan, Critical values in flow patterns of Magneto-Carreau fluid over a circular cylinder with diffusion species: multiple solutions, J. Taiwan Inst. Chem. Eng. 77 (2017) 282–292.
[21] M. Khan, H. Ali and A. Hafeez, A review on slip-flow and heat transfer performance of nanofluids from a permeable shrinking surface with thermal radiation: dual solutions, Chem. Eng. Sci., doi.org/10.1016/j.ces.2017.07.024.
[22] H. Ali, M. Khan, A.S. Alshomrani, Numerical simulation for flow and heat transfer to Carreau fluid with magnetic field effect: dual nature study, J. Magn. Magn. Mater. 443 (2017) 13–21.
[23] H. Ali, M. Khan, A.S. Alshomrani, Characteristics of melting heat transfer during flow of Carreau fluid induced by a stretching cylinder, Eur. Phys. J. E 14 (2017), https://doi.org/10.1140/epje/i2017-11495-6.
[24] A. Bejan, A study of entropy generation in fundamental convective heat transfer, J. Heat Transfer 101 (1979) 718–725.
[25] M. Pakdemirli, B.S. Yilbas, Entropy generation in a pipe due to non-Newtonian fluid flow: constant viscosity case, Sadhana 31 (2006) 21–29.
[26] S. Aiboud, S. Saouli, Entropy analysis for viscoelastic magnetohydrodynamic flow over a stretching surface, Int. J. Non-Linear Mech. 45 (2010) 482–489.
[27] M.M. Rashidi, S. Abelman, N.F. Mehr, Entropy generation in steady MHD flow due to a rotating porous disk in a nanofluid, Int. J. Heat Mass Transfer 62 (2013) 515–525.
[28] N. Galanis, M.M. Rashidi, Entropy generation in non-Newtonian fluids due to heat and mass transfer in the entrance region of ducts, Heat Mass Transfer 48 (2012) 1647–1662.
[29] M.M. Rashidi, A.B. Parsab, O. Anwar Beg, L. Shamekhib, S.M. Sadri, Tasveer A. Beg, Parametric analysis of entropy generation in magneto-hemodynamic flow in a semi-porous channel with OHAM and DTM[1], Appl. Bionics Biomech. 11 (2014) 47–60.
[30] R. Ellahi, M. Hassan, A. Zeeshan, A.A. Khan, The shape effects of nanoparticles suspended in HFE-7100 over wedge with entropy generation and mixed convection, Appl. Nanosci. 6 (2016) 641–651.
[31] M.M. Bhatti, T. Abbas, M.M. Rashidi, M.E. Ali, Numerical simulation of entropy generation with thermal radiation on MHD Carreau nanofluid towards a shrinking sheet, Entropy 18 (2016) 200.
[32] M.Y.A. Jamalabadi, P. Hooshmand, A. Hesabi, M.K. Kwak, I. Pirzadeh, A.J. Keikha, M. Negahdari, Numerical investigation of thermal radiation and viscous effects on entropy generation in forced convection blood flow over an axisymmetric stretching sheet, Entropy 18 (2016) 203.
[33] M.A. Sleigh, The Biology of Cilia and Flagella, MacMillian, New York, 1962.
[34] T.J. Lardner, W.J. Shack, Cilia transport, Bull. Math. Biophys. 34 (1972) 25–35.
[35] W. Yu, S.U.S. Choi, The role of interfacial layers in the enhanced thermal of nanofluids: a renovated Maxwell model, J. Nanopart. Res. 5 (2003) 167–171.
[36] N.S. Akbar, M. Raza, R. Ellahi, Influence of heat generation and heat flux on peristaltic flow with interacting nanoparticles, Eur. Phys. J. Plus 129 (2014).

Please cite this article in press as: M.N. Abrar, et al., ENTROPY ANALYSIS IN A CILIA TRANSPORT OF NANOFLUID UNDER THE INFLUENCE OF MAGNETIC FIELD, Nuclear Engineering and Technology (2017), https://doi.org/10.1016/j.net.2017.09.007